

## **Supplementary Information**

*for*

### **Single Gold Nanostars with Multiple Branches as Multispectral Orientation Probes in Single-Particle Rotational Tracking**

Geun Wan Kim<sup>1</sup> and Ji Won Ha<sup>1,2\*</sup>

<sup>1</sup>Advanced Nano-Bio-Imaging and Spectroscopy Laboratory, Department of Chemistry, University of Ulsan, 93 Daehak-ro, Nam-gu, Ulsan 44610, Republic of Korea

<sup>2</sup>Energy Harvest-Storage Research Center (EHSRC), University of Ulsan, 93 Daehak-ro, Nam-gu, Ulsan 44610, Republic of Korea

\*To whom correspondence should be addressed.

**J. W. Ha**

Phone: +82-52-712-8012

Fax: +82-52-712-8002

E-mail: [jwha77@ulsan.ac.kr](mailto:jwha77@ulsan.ac.kr)

# 1. Supplementary Movies

**Movies S1:** A movie to show the *in-focus* gold nanostar (AuNS) rotating on the glass slide in water. This movie was recorded at 700 nm with the temporal resolution of 100 ms (10 fps).

## 2. Experimental Section

**Synthesis of Gold Nanostars in EPPS Buffer.** The AuNSs were synthesized by a seedless method with a biocompatible Good's buffer. The Good's buffer in the AuNS synthesis negates the need for additional stabilizing surfactants. The Good's buffer plays a dual reducing and shape-directing role in the AuNS production. The AuNSs were synthesized from 4-(2-hydroxyethyl)-1-piperazine propanesulfonic acid (EPPS, Sigma-Aldrich) and gold salt ( $\text{HAuCl}_4$ , Sigma-Aldrich), as described in the literature.<sup>1</sup> To prepare a 20 mL batch of AuNS,  $\text{HAuCl}_4$  (0.2 mL) was added to EPPS buffer (final concentration 100 mM), and the solution was immediately vortexed for 1 min.

**Characterization of the Synthesized Gold Nanostars.** The AuNSs prepared in EPPS buffer were characterized by a TEM (JEL-2100F, JEOL, Japan) and a SEM (JSM-6500, JEOL, Japan). The ensemble extinction spectrum of the AuNSs was obtained by a Varian Carry 300 UV–Vis spectrometer (Agilent Technologies).

**Low-Vacuum SEM in Single-Particle Correlation Study.** We obtained SEM images on nonconductive glass substrates using low-vacuum mode on an FEI Quanta 600F sFEG ESEM. The large-field gaseous secondary electron detector was used to obtain topographical information from samples, where out-of-plane 3D branches produce brighter contrast. We

measured sizes (branch length, core diameter, tip radius of curvature) of AuNS manually from SEM images. The SEM results were correlated with optical images and spectra of single AuNSs. A gold pattern was created by evaporating a 5 nm Ti layer followed by a 20 nm Au layer through an indexed copper transmission electron microscopy (TEM) grid (Ted Pella) placed on the cleaned glasses. Thus, the gold pattern allowed us to locate the exact same nanoparticles throughout this correlation study (Fig. S5).

**Sample Preparations for Single-Particle Microscopy and Spectroscopy.** The samples for single-particle studies were prepared as follows. First, the colloid solution was diluted with 18.2 M $\Omega$  pure water to the proper concentration. The diluted solution was then sonicated for 10 min at room temperature. Samples were prepared by drop-casting the diluted AuNS solution onto pre-cleaned glass slides. This slide was then covered with a 22 mm  $\times$  22 mm No. 1.5 coverslip (Corning, NY, USA). Throughout all experiments, the area density of the AuNSs deposited on the glass slide was maintained at approximately 1.0  $\mu\text{m}^{-2}$  to facilitate single-AuNS characterization, free of inter-particle interactions and LSPR coupling.

**DF Microscopy and Spectroscopy.** The DF microscopy imaging was carried out in an in-house system comprising a Nikon inverted microscope (ECLIPSE Ti-U, Japan), a CCD camera (iXon Ultra 897, UK), and image analysis software. In DF mode, we utilized a Nikon Plan Fluor 100  $\times$  0.5–1.3 oil iris objective and a Nikon DF condenser. The Andor iXon<sup>EM+</sup> CCD camera acquired the DF scattering images of the AuNSs. The collected images were analyzed by Image J software. Furthermore, the DF scattering spectra were acquired by an Andor spectrometer (SHAMROCK 303i, SR-303I-A, UK) and an Andor CCD camera (Newton DU920P-OE, UK). For analysis, the scanning stage was positioned to present the sample at the desired location. Therefore, only the scattered light from the selected location was collected by the objective. The

scattered light was directed to the spectrometer, dispersed by a grating (300 lines/mm), and detected by a Newton CCD camera (Andor, UK). The background spectrum was obtained from a region without particles.

**DIC Microscopy.** DIC microscopy was performed using a Nikon inverted microscope (ECLIPSE Ti-U, JAPAN). DIC microscopy employs a set of two Nomarski prisms, two polarizers, and a quarter-waveplate. The samples were illuminated by an oil-immersion condenser with a numerical aperture (NA) of 1.4. The DIC signals arriving from the sample were collected by a Plan Apo oil-immersion objective (100 $\times$ , NA=1.4). High-quality DIC images were captured by an Andor EMCCD camera (iXon Ultra 897, UK) and were analyzed by Image J and Matlab.

**Preparation of AuNS Rotating at the Glass-Water Interface.** To observe AuNS rotating at the glass-water interface, AuNSs were placed in a gasket between a clean No. 1.5 coverslip and the glass slide. Under this condition, single AuNS attached to and rotated on the coverslip without translation or detachment. 500-frame videos were acquired using bandpass (BP) filters of 640/ $\pm$ 5 nm, 700/ $\pm$ 5 nm, and 750/ $\pm$ 5 nm and exposure time of 100 ms (10 fps).

**Preparation of Synthetic Membrane on Glass Slides.** The phospholipid 1-palmitoyl-2-oleoyl-sn-glycero-3-phosphocholine (POPC, Avanti Polar Lipids) solution in chloroform was first dried by a nitrogen stream and followed by at least 3 hr drying under vacuum at room temperature to remove the residual chloroform. The dried lipids were stored in a -20 $^{\circ}$ C freezer. Phosphate buffered saline (1 $\times$  PBS, pH 7.4) was used to bring the final concentration to 0.5 mg/mL. The cloudy solution containing multilamellar vesicles was obtained after swelling in the PBS buffer solution with several times vortexing. The suspension solution was then forcing through a 100 nm pore size polycarbonate membrane at least 21 times to prepare the solution with large

unilamellar vesicles using a mini-extruder (Avanti Polar Lipids, Alabaster, AL). The resulted solution was kept in a 4°C fridge. The planar bilayer was formed by incubating the large unilamellar vesicles solution on a freshly cleaned glass slide in a chamber created by two double-sided tapes and a clean coverslip for 10 min. After that, PBS was used to remove the excess lipids. AuNS solution was then introduced into the chamber with the membrane for optical imaging.

**Finite-Difference Time-Domain (FDTD) Simulations.** The fundamentals of the FDTD method involve solving Maxwell's equations in the time domain after replacement of the derivatives by finite differences. It has been applied to many problems of propagation, radiation and scattering of electromagnetic waves. In this study, simulations were performed with commercially available software (FDTD Solutions 2016a, Lumerical Solutions Inc.) to provide quantitative predictions of the localized electro-magnetic field distribution as a function of wavelengths of incident light. The AuNS object was designed as a spherical core with conical branches ending in spherical tips with material properties defined by Johnson and Christy.<sup>2</sup>

**Rotational Study under DIC Microscopy.** The sample glass slide was placed on a 360° rotating mirror holder affixed onto the microscope stage. By rotating the mirror holder 10° per step, the AuNSs were positioned in different orientations. DIC images at 640 nm and 750 nm were taken with the Andor EMCCD camera. The corresponding bandpass filters (640/±5 nm, 750/±5 nm) were inserted in the beam path. The collected images were analyzed with MATLAB and NIH ImageJ.

**Determining the Azimuthal Angle  $\phi$  of AuNS in DIC Microscopy.** In DIC microscopy the incident beam is split into two orthogonally polarized beams in the two bright (blue-arrow) and

dark (red-arrow) polarization directions by the first Nomarski prism as shown in Fig. S8. When two beams pass through the specimen, they generate image contrasts for optical path length gradients in the specimen. Therefore, each of the two orthogonally polarized beams generates an independent intermediate image. One such image is shifted laterally by about 100 nm and then overlapped with the other to generate the final interference image.

For anisotropic shape of AuNSs, the two intermediate images are different because the two illumination beams are phase-delayed to different extents, depending on the orientation of the AuNR relative to the two polarization directions. Therefore, the DIC images of AuNSs appear as diffraction-limited spots with disproportionate bright and dark parts and they show different bright and dark intensities depending on the AuNS orientation. The darkest intensity is observed when a AuNS (or branch) is parallel to the dark polarization axis ( $\varphi = 0^\circ$ , blue-arrow). When we rotate a rotational stage by  $90^\circ$ , the darkest intensity of the AuNR changes to the brightest intensity meaning that it is parallel to the bright polarization axis ( $\varphi = 90^\circ$ , red-arrow). The bright and dark intensities are changed periodically as a function of the orientation angle  $\varphi$  and the intensities from bright and dark polarization directions are anti-correlated. The azimuthal angle  $\varphi$  can be determined using the bright or dark intensities of its DIC images collected at the longitudinal LSPR wavelength.

**DIC Polarization Anisotropy.** Two orthogonal intensities from bright and dark polarization directions are obtained in DIC microscopy. The DIC bright intensity of an AuNR is proportional to the fourth power of the sine of the orientation angle  $\varphi$ .<sup>3</sup> In addition, the DIC dark intensity is proportional to the fourth power of the cosine of the orientation angle  $\varphi$ . Therefore, the normalized bright and dark intensities ( $I_{B,N}$ ,  $I_{D,N}$ ) as a function of the azimuthal angle  $\varphi$  can be written as

$$I_{B,N}(\varphi) = \sin^4(\varphi) \quad (\text{Eq. S1})$$

$$I_{D,N}(\varphi) = \cos^4(\varphi) \quad (\text{Eq. S2})$$

DIC polarization anisotropy  $P$  is defined as

$$P = \frac{I_{B,N} - I_{D,N}}{I_{B,N} + I_{D,N}} \quad (\text{Eq. S3})$$

Therefore, the polarization anisotropy  $P$  can be rewritten as

$$P = \frac{\sin^4(\varphi) - \cos^4(\varphi)}{\sin^4(\varphi) + \cos^4(\varphi)} \quad (\text{Eq. S4})$$

The orientation angle  $\varphi$  can be expressed in terms of  $P$  and the following relationship for the orientation angle  $\varphi$  as a function of  $P$  was finally obtained.

$$\varphi = \arccos\left(\sqrt{\frac{A - \sqrt{A^2 - 2A}}{2}}\right), \quad P < 0 \quad (\text{Eq. S5})$$

$$\varphi = \arccos\left(\sqrt{\frac{A + \sqrt{A^2 - 2A}}{2}}\right), \quad P > 0 \quad (\text{Eq. S6})$$

where  $A$  is defined as  $(P-1)/P$ .

**Measuring AuNS at Multiple Wavelengths in DIC Microscopy.** As a control experiment, we measured Au nanospheres with an average diameter of 100 nm (LSPR peak: 540 nm) and gold nanorods (AuNRs) with an average size of 25 nm × 73 nm (Longitudinal peak: 700 nm). AuNS can be measured with high contrast at multiple wavelengths, and DIC images changed depending on a branch that is excited at the illumination wavelength (e.g., bright to dark image) (Figs. S15a-c). Au nanospheres, however, can be measured at their one LSPR wavelength of 540 nm. Anisotropic AuNRs can also be measured with high contrast at their longitudinal LSPR wavelength of 700 nm (Figs. S15d-f).

**Comparison of AuNS with Conventional AuNR as Orientation Probes.** A major advantage of using AuNSs is that, unlike Au nanorods, single AuNSs can be used as multispectral orientation probes that can provide detailed information such as rotational motions and rotational speeds at different branches. However, a major disadvantage is that the synthesized AuNSs are heterogeneous in their morphology (the size and shape, the number of branches, etc.). Thus, the heterogeneity issue needs to be solved at the end, such as AuNRs.

### 3. References

- 1) Chandra, K.; Culver, K. S. B.; Werner, S. E.; Lee, R. C.; Odom, T. W., Manipulating the Anisotropic Structure of Gold Nanostars using Good's Buffers. *Chemistry of Materials* **2016**, *28* (18), 6763-6769.
- 2) Johnson, P. B.; Christy, R. W., Optical constants of transition metals: Ti, V, Cr, Mn, Fe, Co, Ni, and Pd. *Physical Review B* **1974**, *9* (12), 5056-5070.
- 3) Ha, J. W.; Sun, W.; Wang, G.; Fang, N., Differential interference contrast polarization anisotropy for tracking rotational dynamics of gold nanorods. *Chemical Communications* **2011**, *47* (27), 7743-7745.

## 4. Supplementary Figures

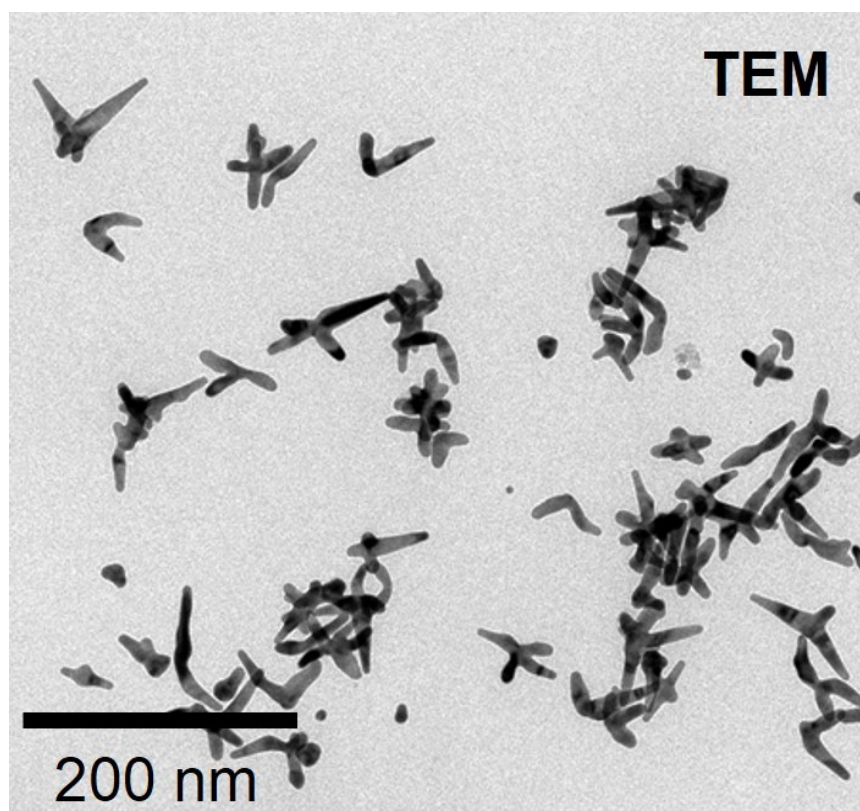


**Fig. S1** A TEM image of AuNS prepared with EPPS. The scale-bar represents 200 nm.

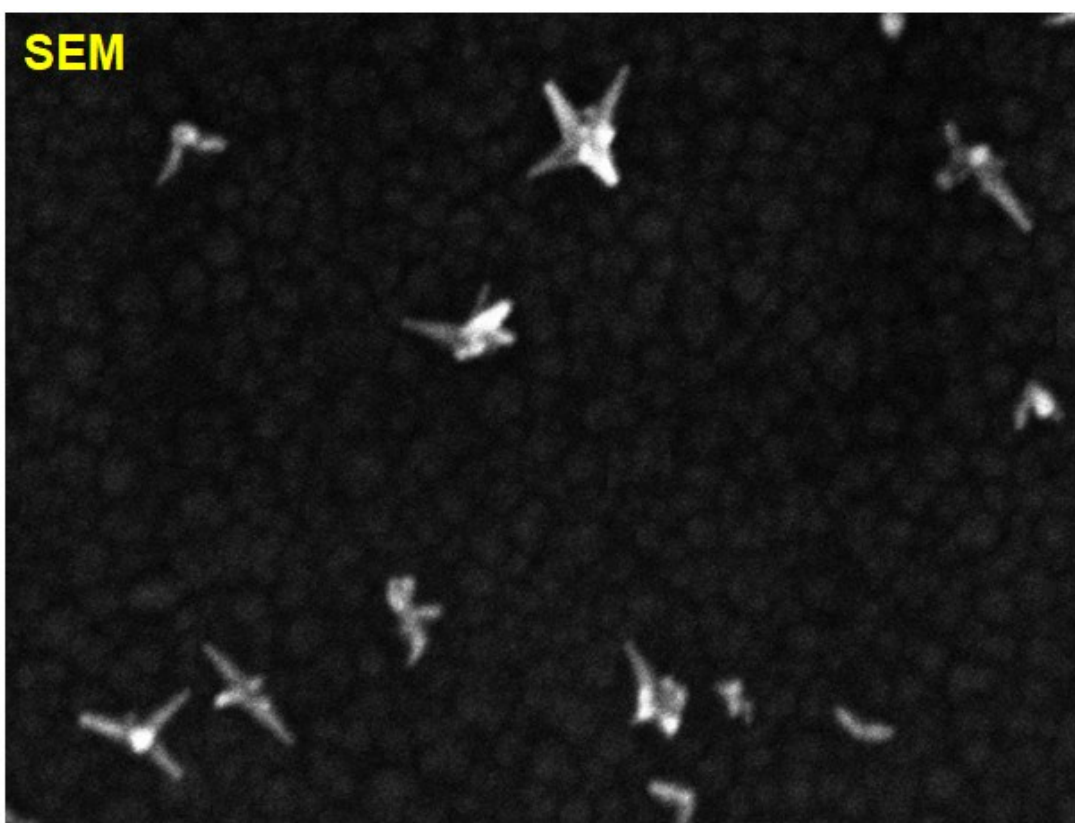


**Fig. S2** SEM image of AuNS prepared with EPPS. The long and sharp branches are observed for the EPPS AuNSs.

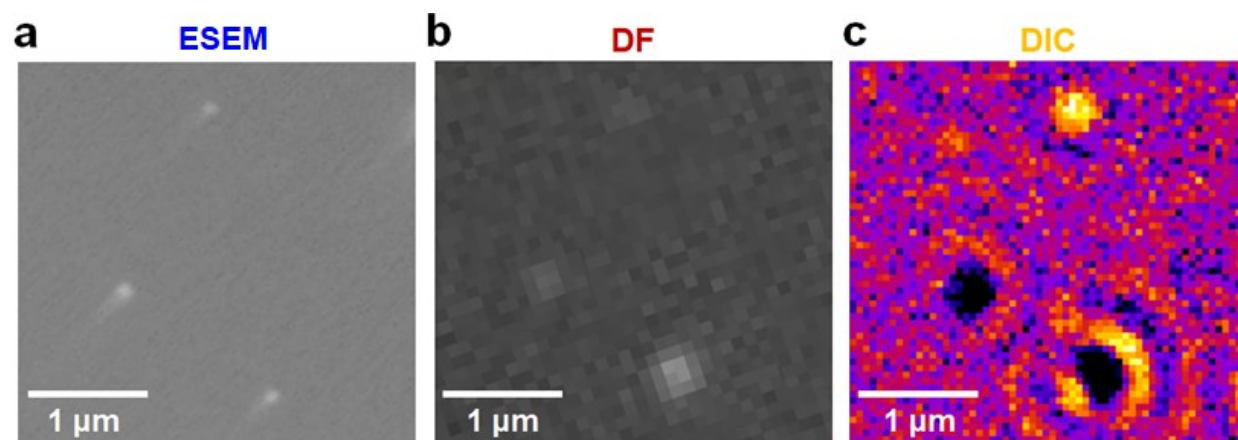


**Fig. S3** A single particle correlation study for the same AuNSs with (a) ESEM image, (b) DF scattering image, and (c) DIC image at 640 nm.

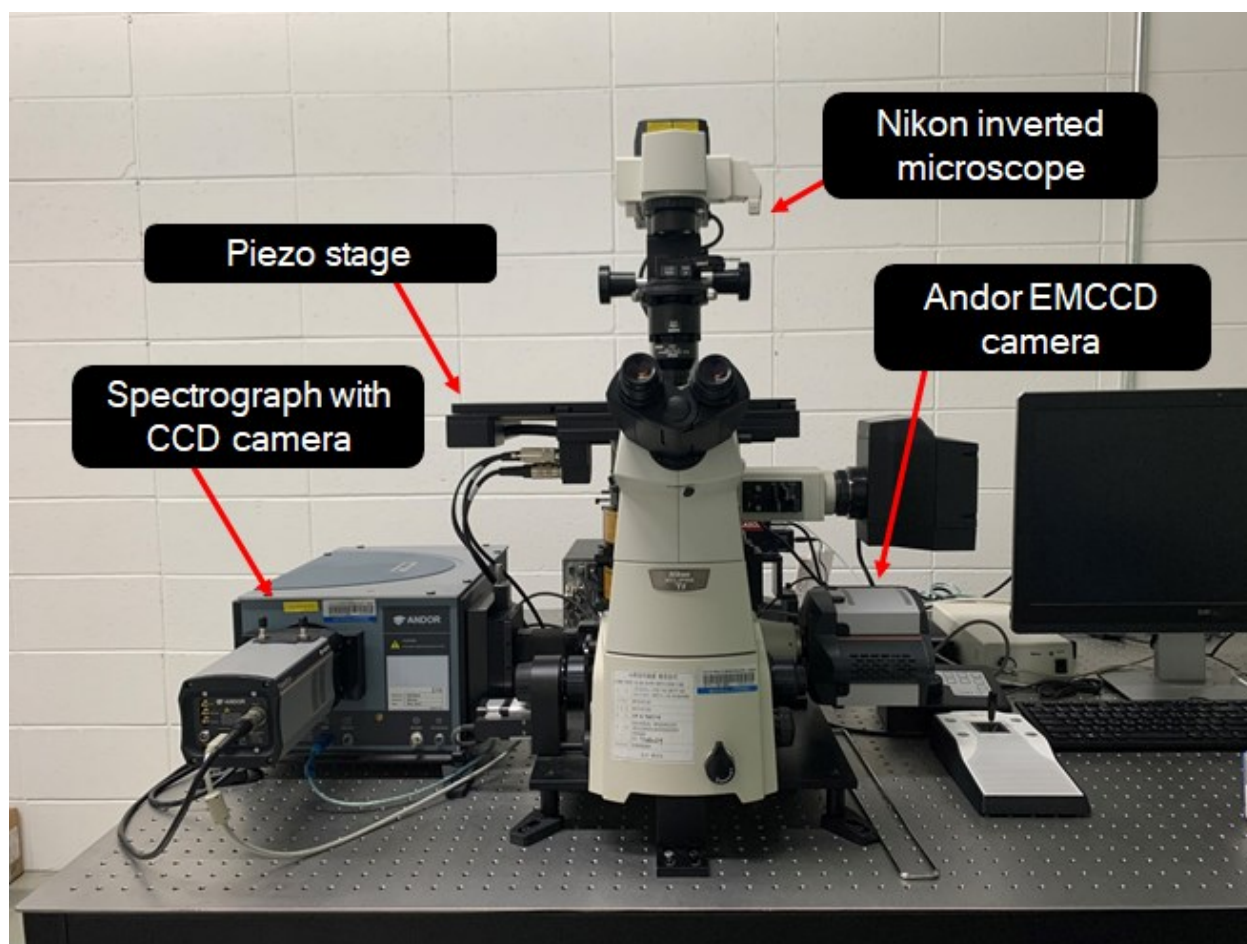


**Fig. S4** Photograph showing the experimental setup for single particle microscopy and spectroscopy.

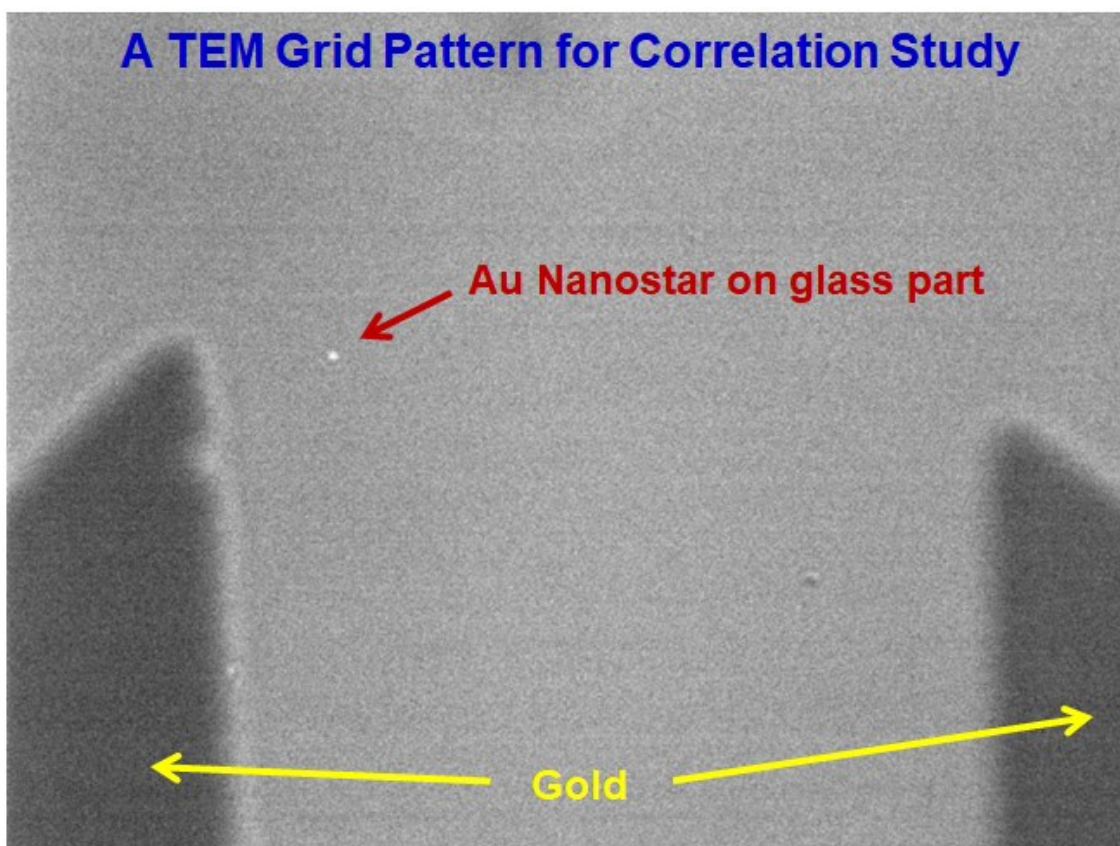


**Fig. S5** A glass slide with a TEM grid pattern used for locating the exact sample AuNSs in this single-particle correlation study. The AuNSs deposited on a glass slide were measured in this study.

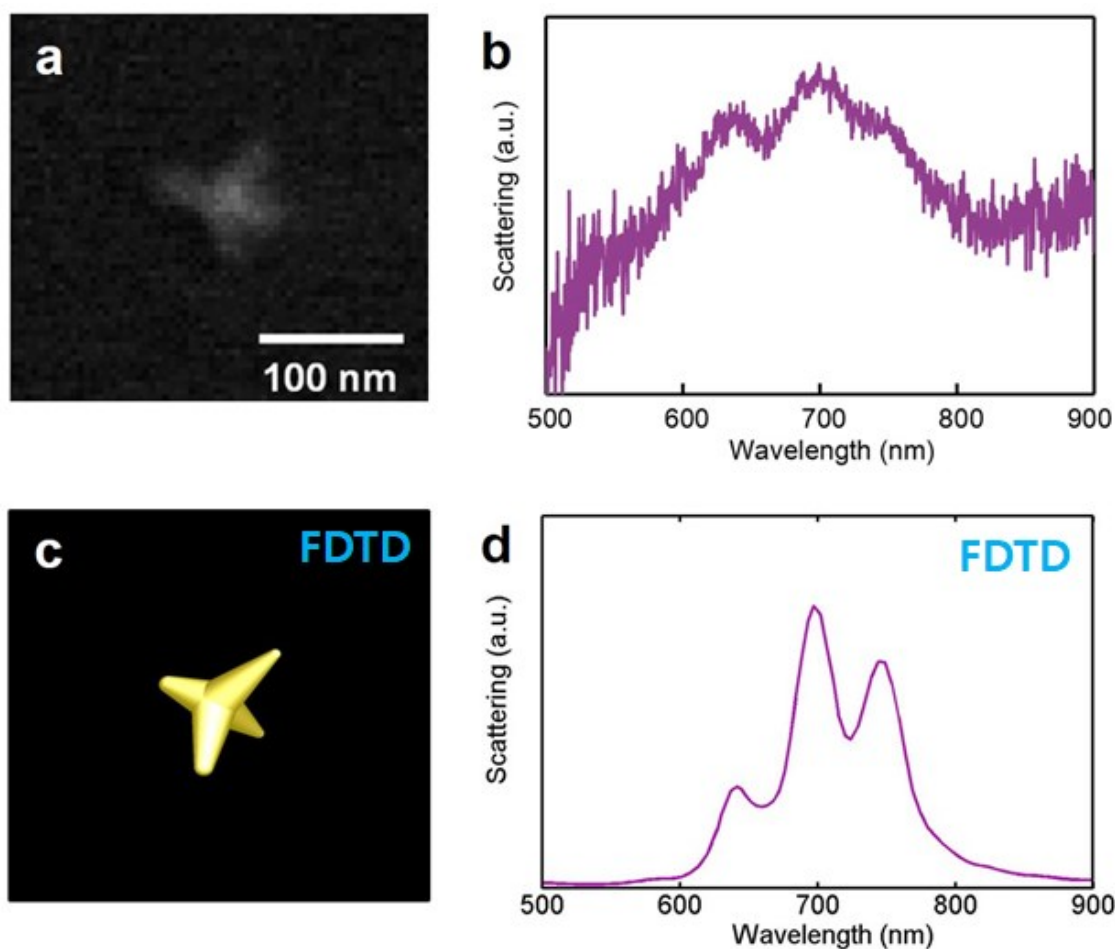


**Fig. S6** (a) ESEM image of a AuNS with different shape. (b) Experimental scattering spectrum. Three SPR peaks are observed for the AuNS at around 640 nm, 700 nm, and 750 nm. (c) FDTD modeled image used for the simulation of a AuNS in (a). (d) Scattering spectrum of the AuNS obtained from the FDTD simulations.

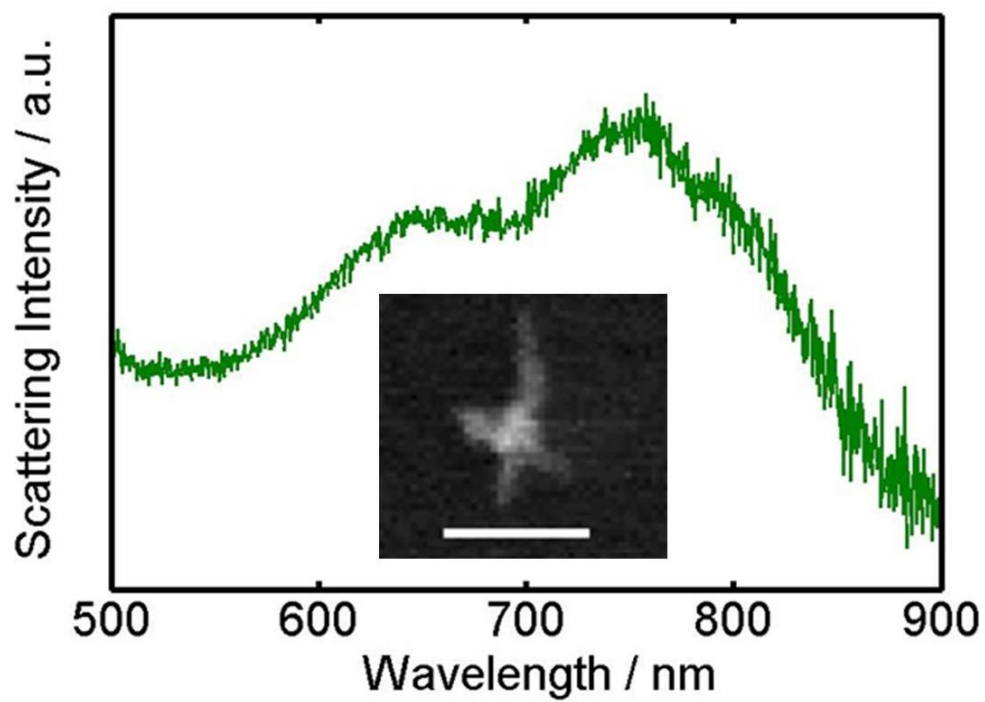


**Fig. S7** Experimental scattering spectrum of a AuNS. Three SPR peaks are observed for the AuNS at around 640 nm, 750 nm, and 780 nm. ESEM image of a AuNS is shown in the inset.

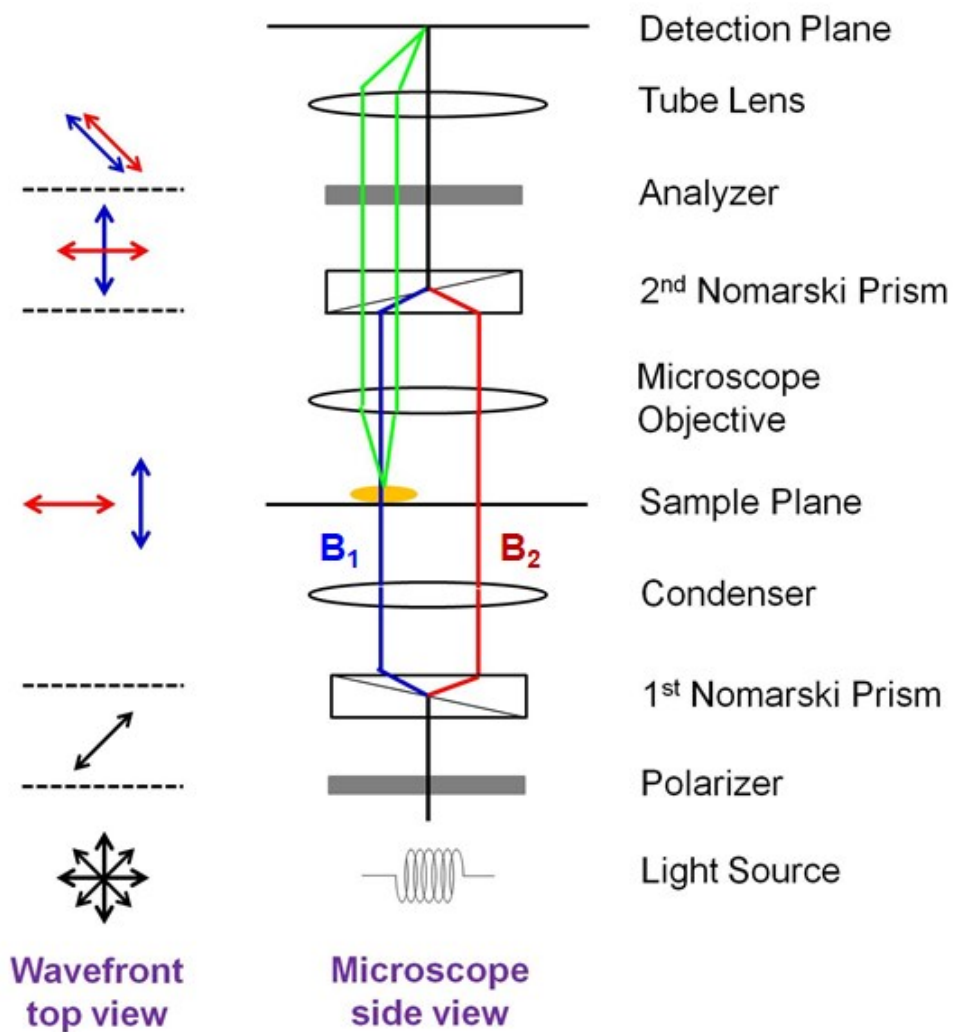


**Fig. S8** Working principle of DIC microscopy. The green line shows scattering contribution to a final DIC image of AuNS.

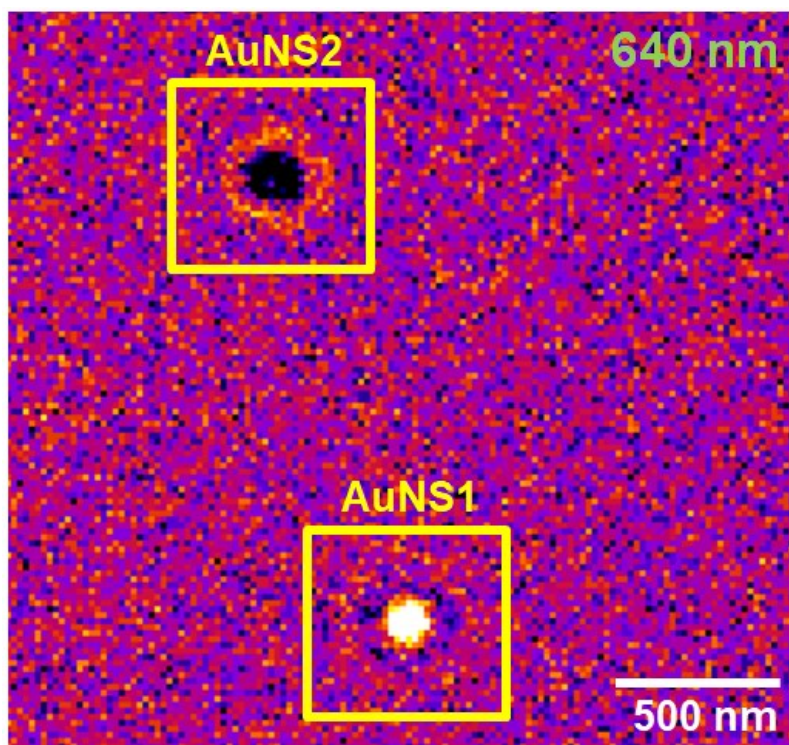


**Fig. S9** DIC image of two AuNSs (AuNS1 and AuNS2) measured at 640 nm. The different DIC image patterns indicate their different orientations.

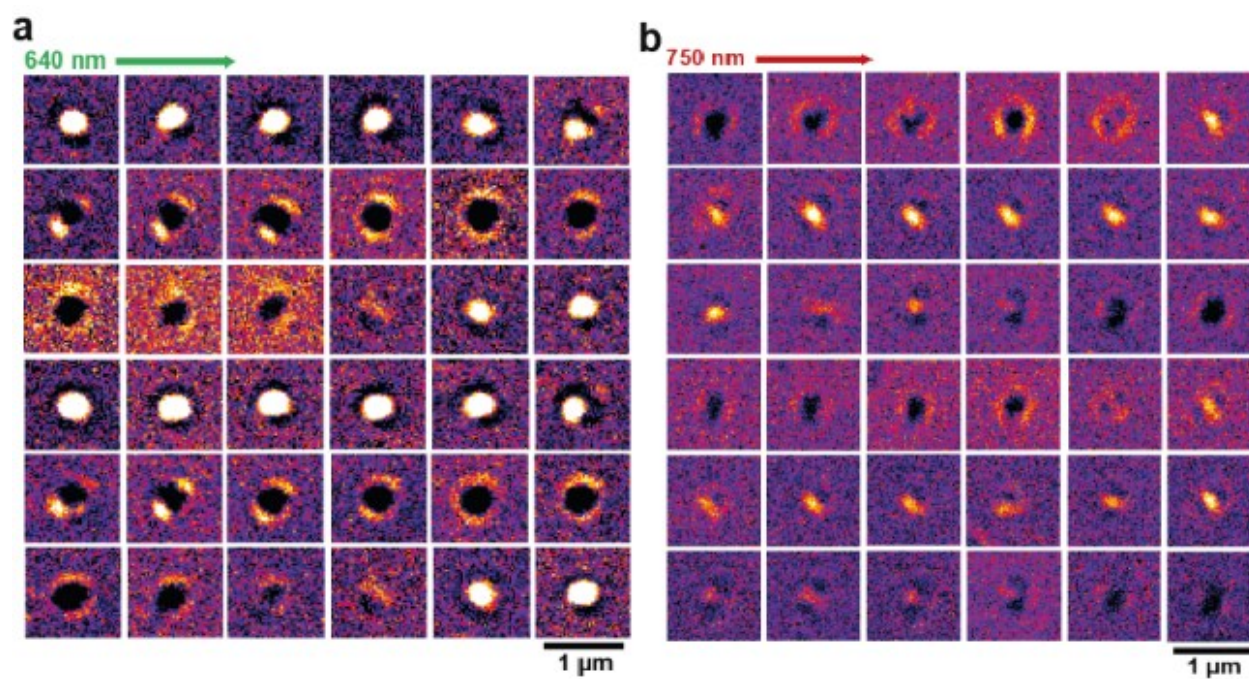


**Fig. S10** A complete set of DIC images of the AuNS1 in Fig. 3 from 0° to 360° for the two LSPR wavelengths of (a) 640 nm and (b) 750 nm with a 10° increment.

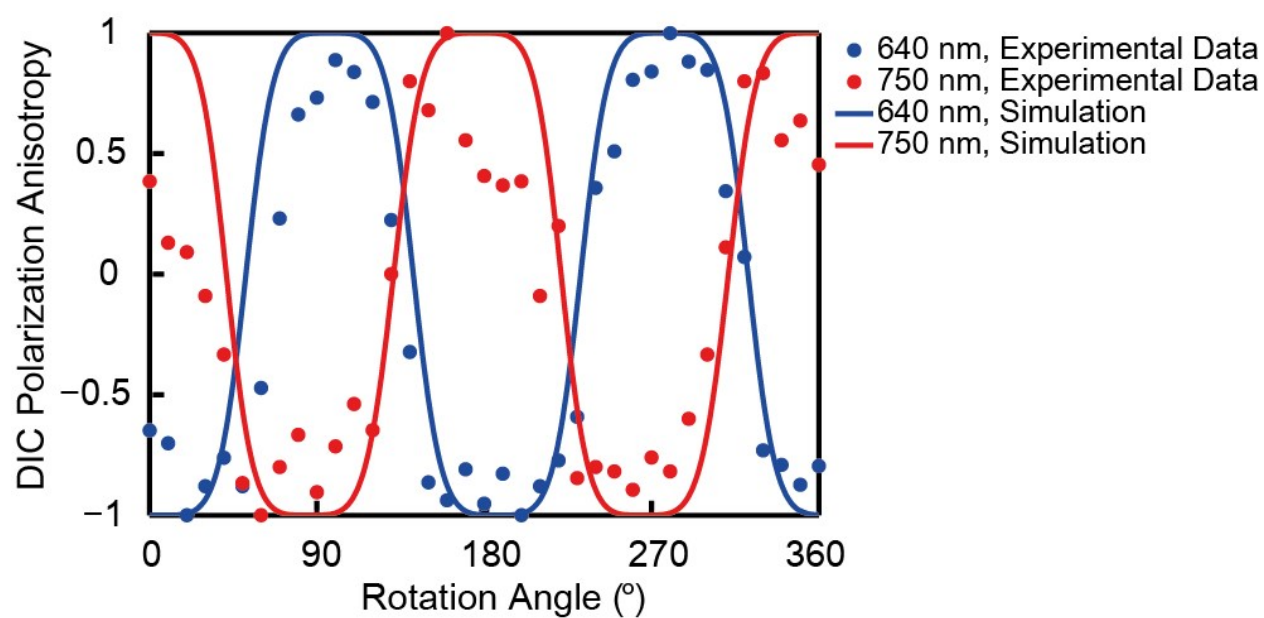


**Fig. S11** DIC polarization anisotropy for two LSPR wavelengths of 640 nm and 750 nm for a AuNS1 in Fig. 3. The experimental data is fitted well with the calculated data.

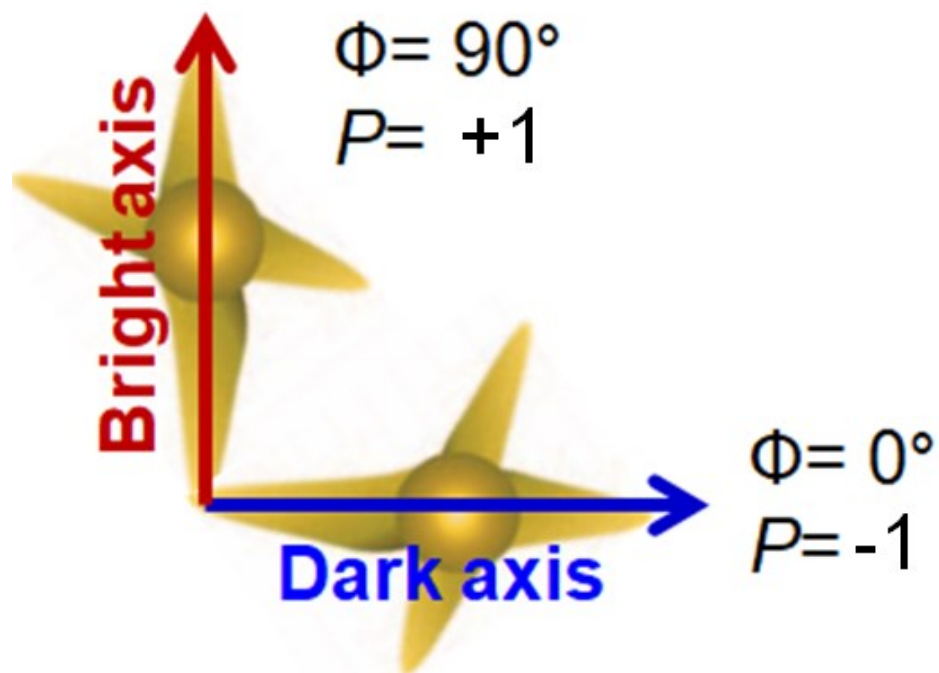


**Fig. S12** Schematic to explain the DIC polarization anisotropy  $P$  values of +1 and -1.  $P$  is going to be -1 when a AuNS is aligned with dark axis (blue-line), whereas  $P$  is going to be +1 when a AuNS is rotated by  $90^\circ$ .

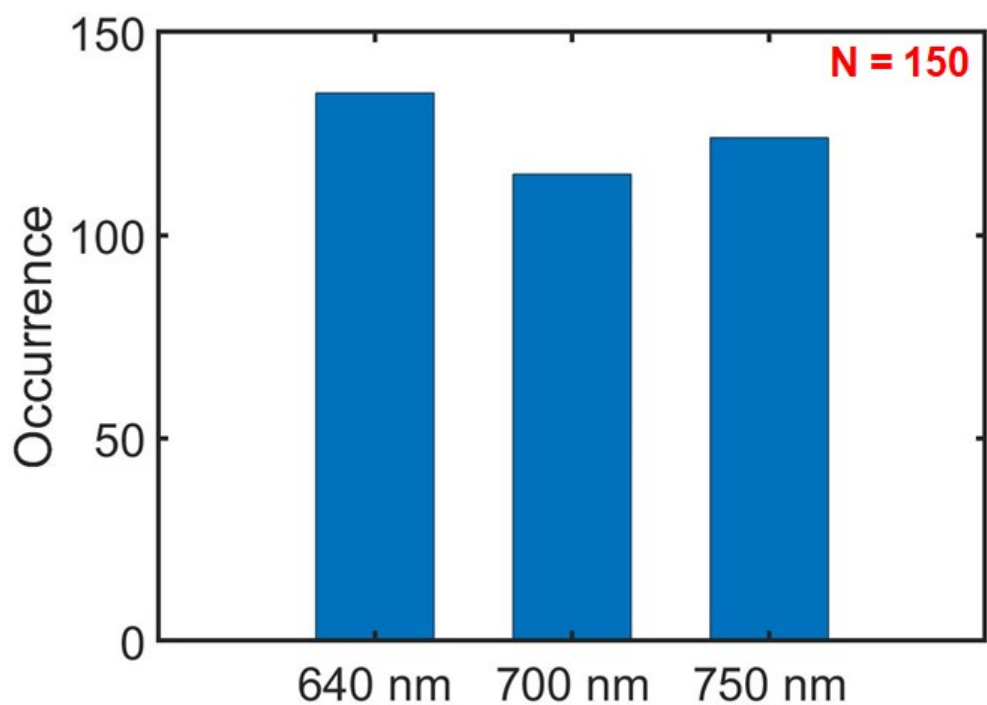


**Fig. S13** Analysis of the LSPR peaks in single particle scattering spectra of AuNSs (N=150). We noticed that the prominent LSPR wavelengths appear mainly in between 620 nm and 750 nm. In particular, the LSPR peaks of single AuNSs prepared in this study using EPPS buffer were mainly observed at about 640 nm, 700 nm and 750 nm. Thus, the probability of finding the LSPR peaks in the three chosen wavelengths were analyzed for 150 single AuNSs.

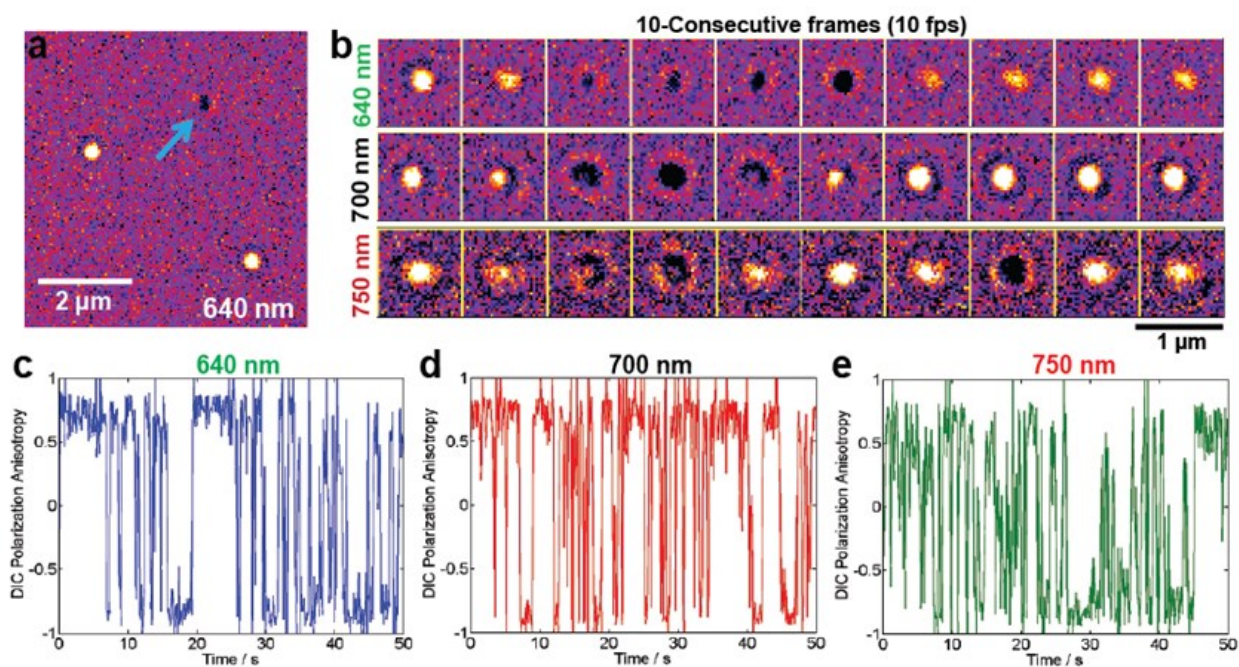


**Fig. S14** Single AuNS as multi-spectral orientation sensors in dynamic studies. **(a)** DIC image of three AuNSs measured at 640 nm in water. Two AuNS are fixed while one AuNS (blue arrow) rotating on a glass slide in water. **(b)** 10-successive DIC images of the AuNS (blue-arrow) in (a) at three chosen wavelengths of 640 nm, 700 nm and 750 nm as a function of time. The 10 images are randomly chosen from a movie at each wavelength. The temporal resolution is 100 ms. **(c-e)** DIC polarization anisotropy of the AuNS under (c) 640-nm excitation, (d) 700-nm excitation, and (e) 750-nm excitation.

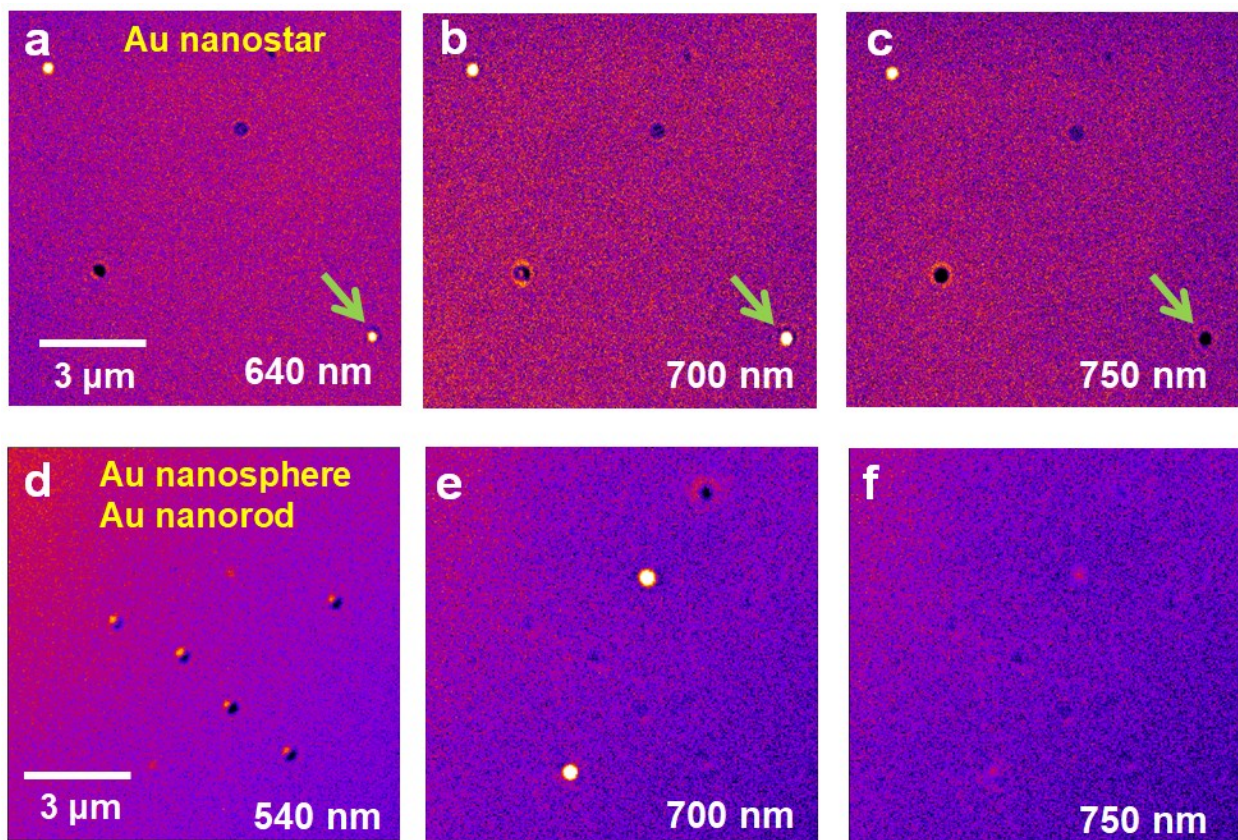


**Fig. S15** AuNS as multi-spectral orientation sensor. **(a-c)** AuNS can be measured with high contrast at three different excitation wavelengths of 640 nm, 700 nm, and 750 nm. **(d-f)** Au nanospheres and AuNRs can be measured at only one LSPR wavelength with high contrast.

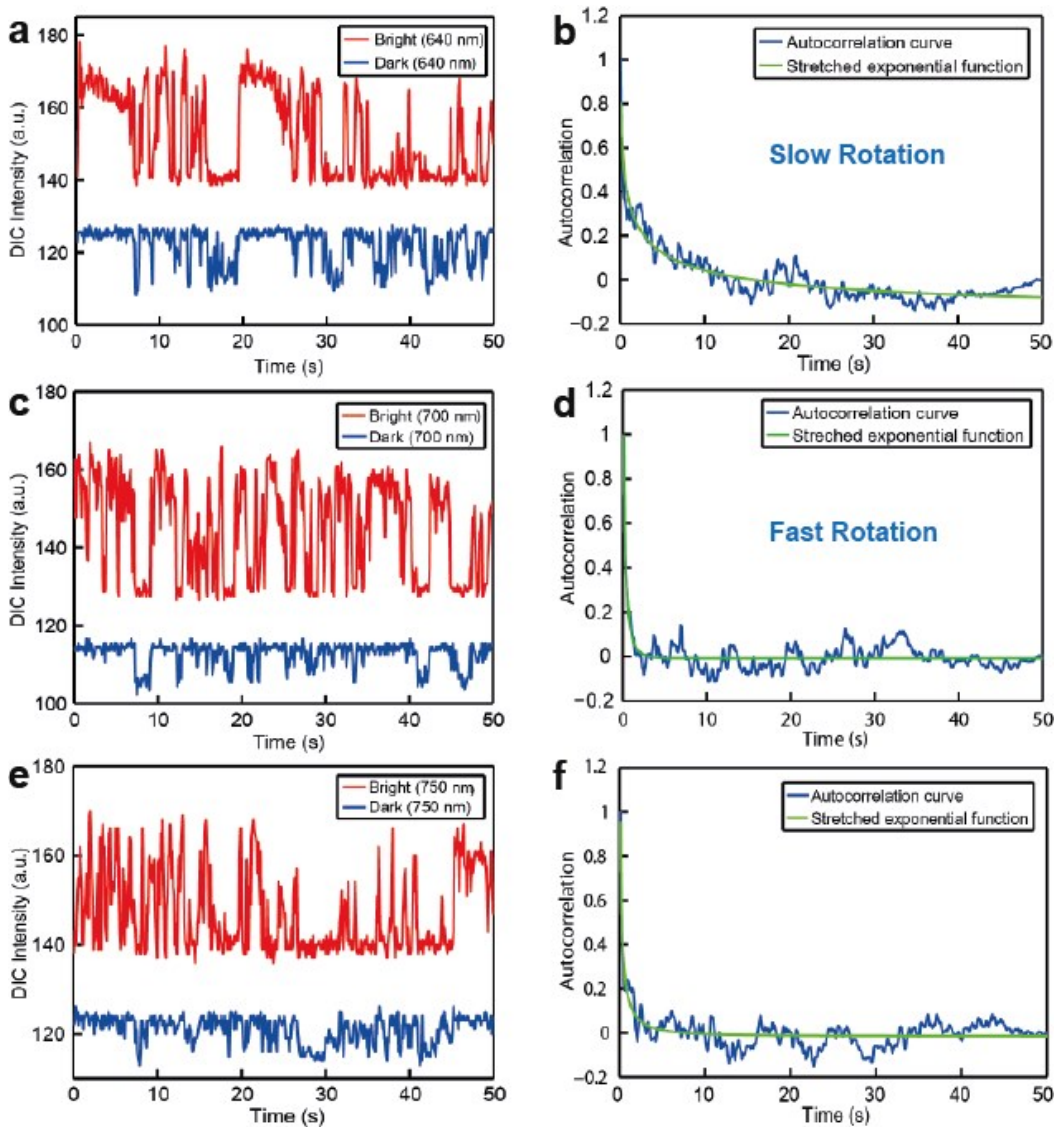


**Fig. S16** Autocorrelation analysis of rotational speed of multi-spectral AuNS. **(a, c, e)** Change in the bright and dark intensities of a rotating AuNS3 (Fig. 4) at the three wavelengths of (a) 640 nm, (c) 700 nm, and (e) 750 nm. **(b, d, f)** Autocorrelation curves for (b) 640 nm, (d) 700 nm, and (f) 750 nm. The mean relaxation times of 6.7 s (slow rotation) at the 640-nm excitation, 0.25 s (fast rotation) at the 700-nm excitation, and 0.11 s at the 750-nm excitation were obtained through nonlinear least-squares fitting.

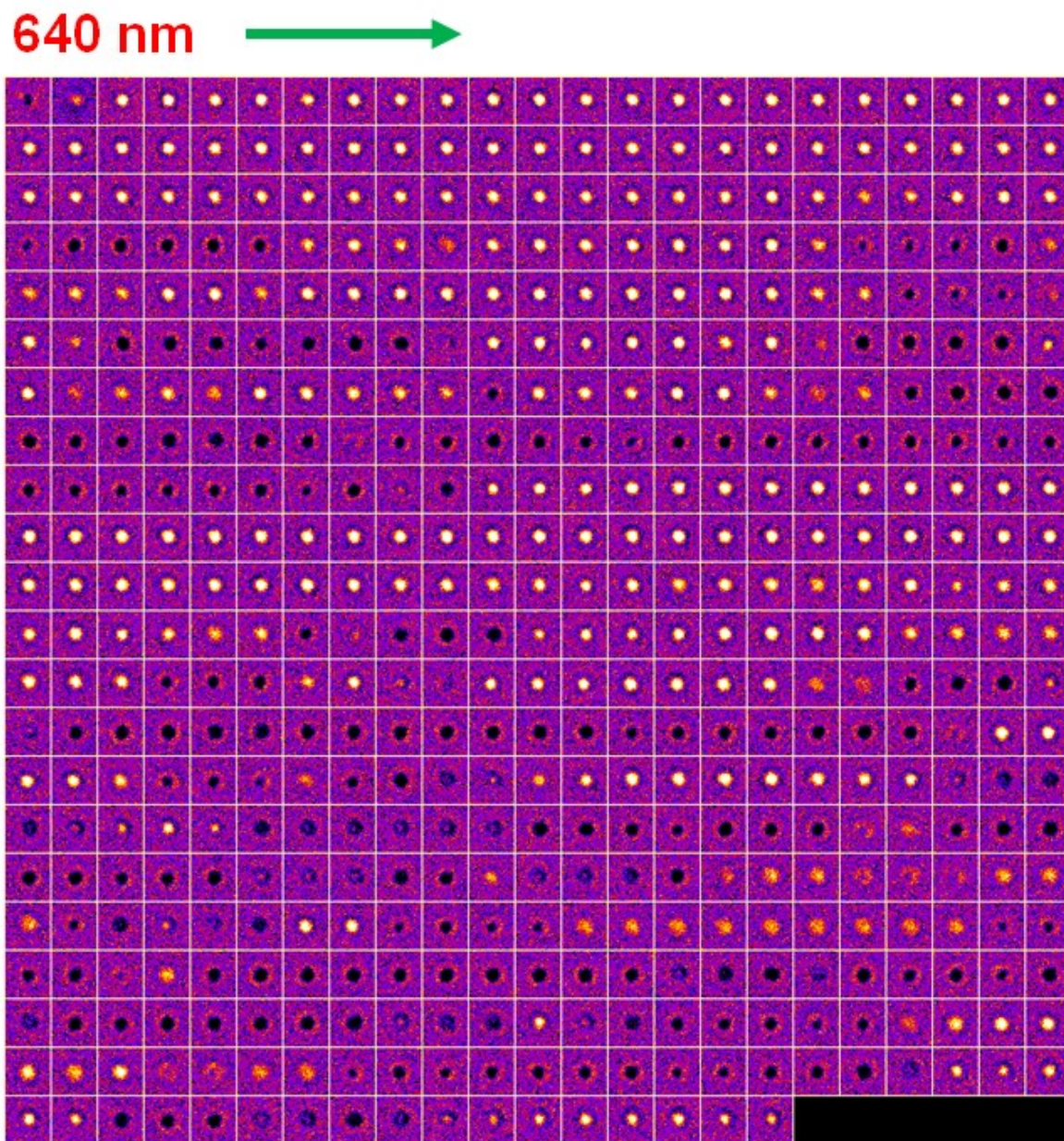
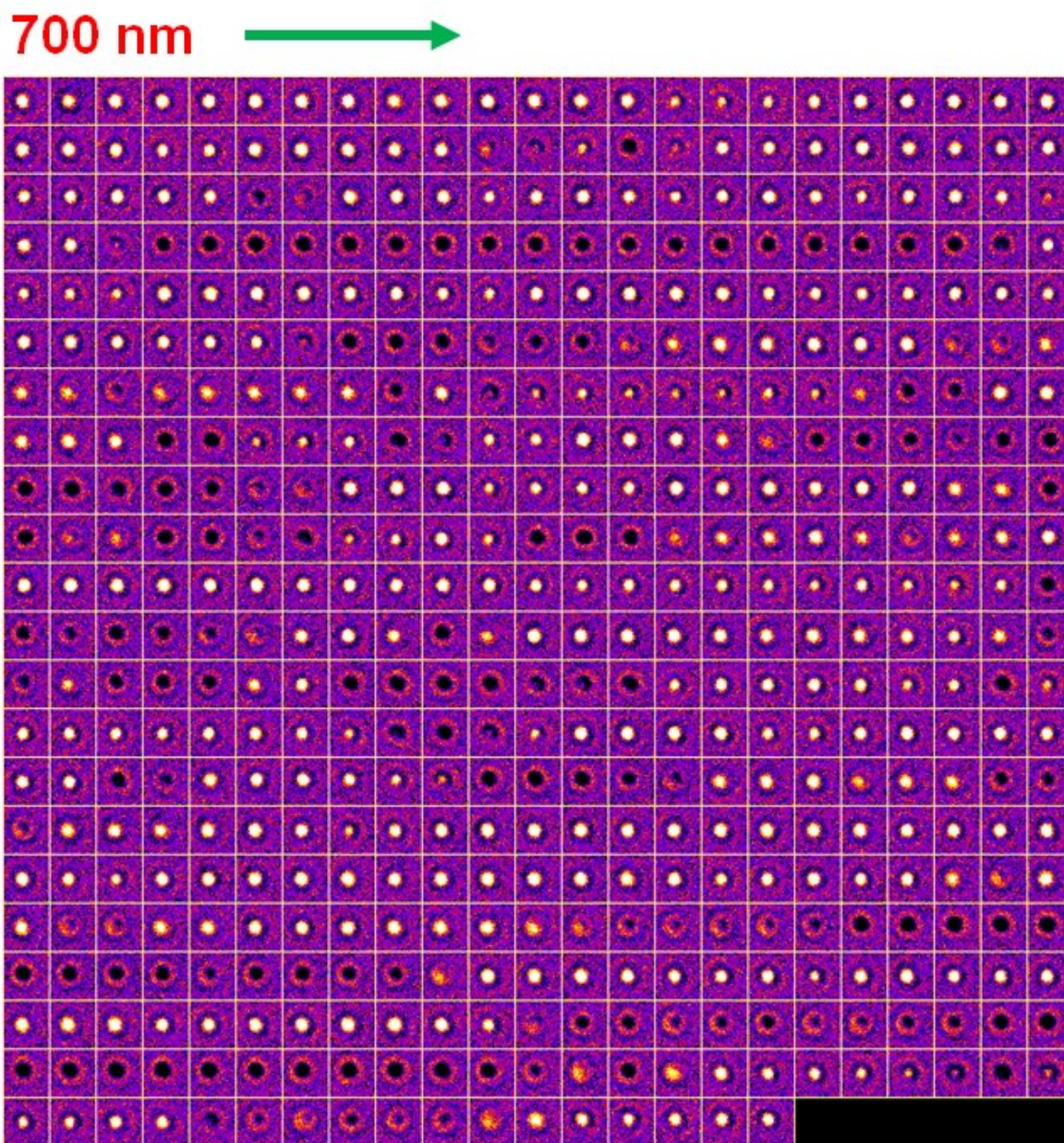
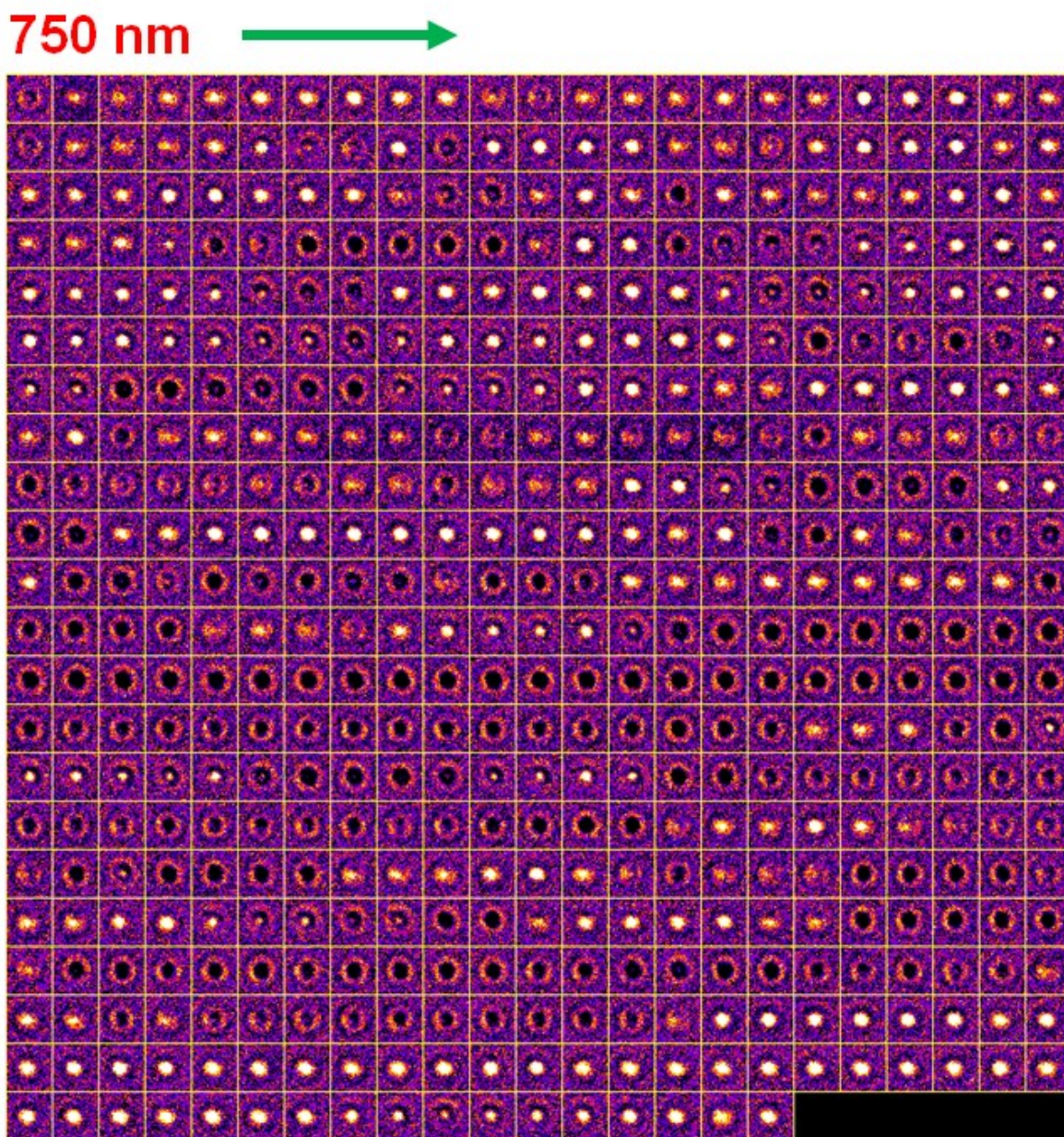


Fig. S17 500-consecutive DIC images of AuNS3 in Fig. 4, which is measured at 640 nm.



**Fig. S18** 500-consecutive DIC images of AuNS3 in Fig. 4, which is measured at 700 nm.



**Fig. S19** 500-consecutive DIC images of AuNS3 in Fig. 4, which is measured at 750 nm.